



Longshore currents on a meso-tidal beach of Goa, India - Measurements and improved formulae

E M Yadhunath^{a,b}, J K Seelam^{*,c,d}, P S Pednekar^c, R K Rajive^{c,e} & R Gowthaman^c

^aBharathidasan University, Tiruchirappalli, Tamil Nadu – 620 024, India

^bNaval Physical and Oceanographic Laboratory, Thrikkakara, Kerala – 682 021, India (Present address)

^cCSIR-National Institute of Oceanography, Dona Paula, Goa – 403 004, India

^dAcademy of Scientific and Innovative Research, Ghaziabad – 201 002, India

^eCochin University of Science and Technology, Cochin – 682 022, India (Present address)

*[E-mail: jay@nio.org]

Received 23 February 2021; revised 2 November 2022

Field experiments in the surfzone were conducted on a meso-tidal beach stretch between Sinquerim and Baga off Goa on India's central west coast. Surfzone waves and currents were measured using an array of seabird wave and tide gauges and Aanderaa RCM9 current meters. Rip currents were observed prominently in this stretch with increased intensity during the ebb tide. Six longshore current prediction equations are tested for their suitability in this region. The Longshore Current (LSC) estimated using these equations showed a wide range of Mean Absolute Percentage Error (MAPE) and Scatter Index, and the correlation coefficients were also found to be less than 50 %. Hence, these equations are further modified by including the alongshore wind shear component, and the LSC was re-estimated to study the variations in current along the Candolim beach. It was observed that the correlation coefficients improved up to 64 % for most of the equations.

[**Keywords:** Longshore currents, Rip currents, Surfzone, Waves]

Introduction

Investigations on surfzone currents, including longshore currents, rip currents, and nearshore circulation, have been conducted worldwide since 1920. Reniers & Battjes¹ termed longshore current as the time-averaged current which flows alongshore between the first breaker and shoreline. Guza & Thornton² concluded that "An appropriate temporal averaging time for a mean longshore current is not known". Published studies regarding longshore currents are aimed at developing a method to predict longshore current velocity. As a result of this, different researchers developed different equations based on different principles and approaches. Variables used to estimate Longshore Currents (LSC) in those equations are obtained from the field or laboratory, which include a mean longshore current velocity (V), wave height (H), wave direction (Θ), period (T), and beach slope (m). Most preferable laboratory studies for computing longshore current were Putnam *et al.*³, Saville⁴, Brebner & Kamphuis⁵, and Galvin & Eagleson⁶.

Galvin⁷ described generating LSC and predicted the equation for the velocity of currents and

experimental verification for this prediction, and finally investigated the relation between longshore current and sediment transport. Longshore currents estimated by different theories using the variables from laboratory data showed significant differences compared to the float and dye method. During one test, the velocity observed by Galvin & Eagleson⁶ is 70 % higher than that by Brebner & Kamphuis⁵ and 28 % larger than the velocity observed by Putnam & Munk³. Inman & Quinn⁸ have averaged the measured data at 90 m intervals along the beach, but local conditions do not exactly resemble the average conditions along the beach in this study. Harrison⁹ subjected a multi-regression analysis and suggested that estimated LSC velocity has a prime dependence on wave breaker angle than the period, breaker height and beach slope. Longuet-Higgins¹⁰ [here after, referred to as LH70] used the concept of radiation stress for obtaining longshore current velocity equation as a function of distance from swash line together with eddy viscosity. Brebner & Kamphuis⁵ suggested that the angle made by the breaker crest at deep water and the breaker angle are the major sources providing energy to the longshore current

generation. Komar & Inman¹¹ proposed a solution for longshore current velocity prediction based on Longuet-Higgins¹⁰; whereas, Komar & Inman¹¹ used an empirical relationship considering the horizontal orbital velocity due to prevailing breaking waves.

Lanfredi & Framinan¹² suggested that for predicting longshore current velocity, the most important variables are the angle of incidence of the incoming waves and an alongshore component of wind velocity. After including the wind effects in Longuet-Higgins¹⁰ and Komar & Inman¹¹ formulae, a better fit between observed and predicted current velocities were observed. Nummedal & Finlay¹³ did a statistical analysis to understand the influence of wind stress on longshore current generation. But based on a recent laboratory study on LSC¹⁴, it is concluded that location-specific beach morphology and wave climate modifies the characteristics of LSC, hence suggested that the time-dependent three-dimensional models of waves and currents can be used to predict LSC rather than using the wave and depth-averaged radiation stress concept.

Longshore current velocity can practically be predicted with the wave data and beach topography using the methods discussed above. However, studies on LSC and its prediction along the Indian coastline are limited. Among the notable works in India, Kumar *et al.*¹⁵ compared measured data from Kannirajapuram coast, Tamil Nadu. They observed that LH70 overpredicts by 32 %; whereas, Galvin overpredicts by 6 %. However, Hameed *et al.*¹⁶ revealed that the modified LH70 and Komar equations could give a better correlation for the LSC based on the studies carried out for the Valiyathura and Aleppey coasts, Kerala. Chandramohan *et al.*¹⁷ showed that LH70 gave 25 % higher values than Galvin for the data collected between Ratnagiri and Mangalore coasts, India.

Yadhunath *et al.*¹⁸, measured the longshore current using AANDERAA RCM9, and wave parameters were measured using a Seabird wave and tide gauge for 2 h at the inner surfzone of Candolim and Miramar beaches of Goa. Instruments were deployed at the surf zone of depth 0.5 m, in which RCM9 was buried inside the seabed with a sensor head placed above the seabed. These measured currents were compared with eleven theoretical equations by applying the measured wave data. They observed that with modified coefficients, the LH70 and Komar equations could predict better results with a

magnitude range from 5 – 10 % lesser than the measured velocity. The study based on this 2 h data from a single point was not enough to identify the performance of the general equation's performance. The measurements were carried out at one point location for the 2 h in the rising tide. There were no other parameters available: wind, tide and offshore wave data to relate the findings.

The present study includes measurements of wave and wind parameters at 15 m water depth and deployment of current meters and wave and tide recorder for four consecutive days. The current meters were placed 20 m apart in the alongshore direction in the surf zone. This study aims to understand the variation in the surfzone current velocity and direction over a period and to improve the existing equations being used for the LSC estimation by including the measured wave parameters, wind, and beach slope.

Materials and Methods

Study area

The study area selected on India's central west coast, off Goa state, covers a stretch of 7 km long beach between Sinerim Beach on the south and Baga Beach in the north (Fig. 1). This coastal stretch is the most visited region and most of the fatalities related to beach drowning occurred in this region. The morphology and wave climate of Candolim, Calangute, and Baga within the study region are different. Chandramohan *et al.*¹⁹, observed that during the southwest monsoon, breaking wave heights exceed 2.5 m at Candolim, whereas at other beaches, it is around 1.5 m. Candolim Beach has a well-developed backshore with prominent berm than Calangute; also, Candolim Beach is steeper than Calangute. Earlier studies carried out relating to longshore currents and the occurrence of rip currents at this beach stretch were based on the LEO method^{19,20}.

Methodology

A field experiment was carried out to estimate the LSC velocity in the surfzone. The Directional Wave Rider Buoy (DWRB) was deployed off the Calangute Beach at a water depth of 15 m, for measuring the wave parameters (Fig. 1a). An automatic weather station was mounted on the fishing boat near the DWRB for measuring the wind speed and direction. During this measurement period, a Wave and Tide Gauge (WTG) was deployed at 1.45 m water depth at the location W1, and another array of two RCM

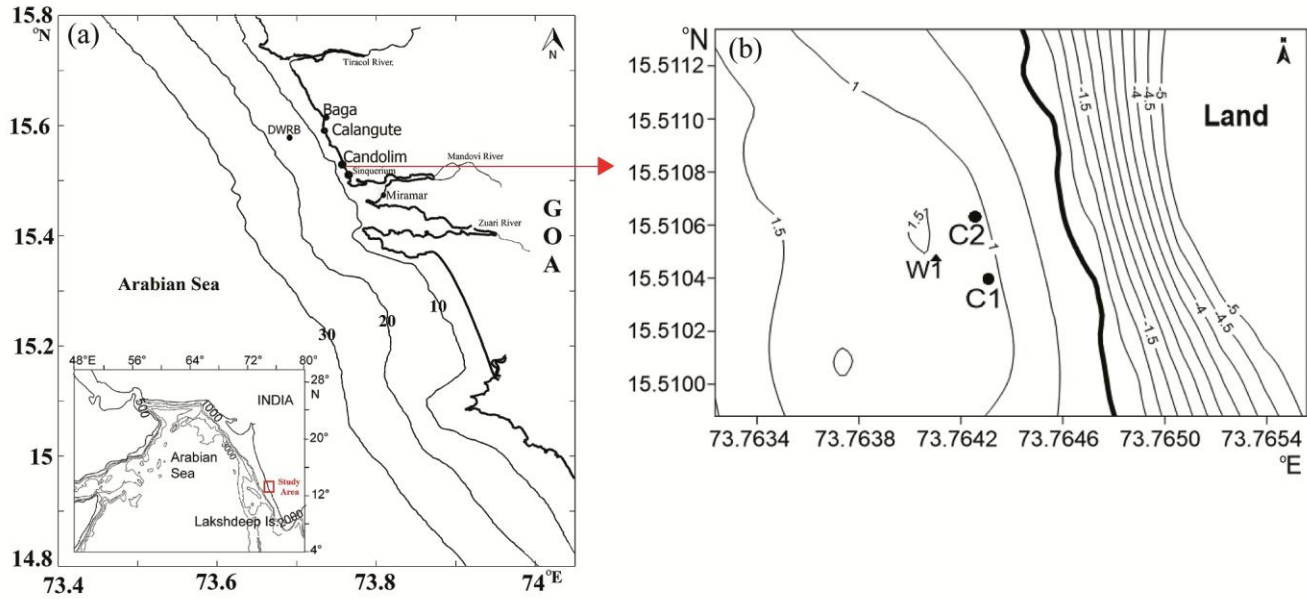


Fig. 1 — Map of (a) Study area, and (b) Measurement locations

Table 1 — Theoretical and empirical formulas used in the study

ID	Author	Formulae	Parameters	The basic scheme of analysis
LH1	Longuet-Higgins modified ¹⁰	$V = 20.7 s (g H_b)^{\frac{1}{2}} \sin(2\alpha_b)$	m = slope	Momentum radiation stress
PMT1	Putnam, Munk & Traylor ³	$V = \frac{a}{2} \left(\sqrt{1 - \frac{4C \sin \alpha}{a}} - 1 \right)$ $a = (2.61 H m \cos \alpha) / K T$	m = slope, K = 0.0078, breaking wave velocity $C = \sqrt{2.28 g H_b}$	Momentum
IQ1	Inman & Quinn ⁸	$V = \left[\left(\frac{1}{4X^2} + C \sin(\alpha_b) \right)^{\frac{1}{2}} - \left(\frac{1}{2X} \right) \right]^2 c$ $X = 108 \frac{H_b}{T_b} m \cos \alpha_b$	$C = \sqrt{2.28 g H_b}$	Momentum
KO1	Komar ¹¹	$V = 2.7 U_m \sin \alpha_b \cos \alpha_b$ $U_m = \frac{1}{2} \gamma_b (g H_b)^{1/2}$	U_m = Maximum wave orbital velocity $\gamma_b = H_b/h_b = 0.78$	Empirical
GA1	Galvin ⁶	$V = K g m T \sin(2 \alpha_b)$	K = 1	Continuity
HA1	Harrison ⁹	$\bar{v} = -0.170455 + 0.0317376(\alpha_b) + 0.031801(T_b) + 0.241176(H_{bs}) + 0.030923(\bar{m})$	\bar{m} is slope	Multiple regression

current meters was also deployed at 1.1 m depth at locations - C1, and C2, off the Candolim Beach (Fig. 1b) from 21st January to 25th January 2017, parallel to the shore.

The WTG provides waves at an interval of every 20 min, and the RCM9 current meters were configured to measure currents every 10 min. The beach face slope is also measured from the beach profile data collected during this period. These measured data is used to estimate the

longshore current velocity from the equations available in the literature (Table 1). The wave breaker angle is one of the significant factors in the theoretical equations, but it isn't easy to measure by any deployed instruments. Hence to get the breaker angle for the study area the direct method of Larson *et al.*²¹ is implemented, wherein the breaker angle is $\theta_b = \arcsin(\sin \theta_m \sqrt{\lambda})$, Where, θ_m is the wave approaching angle towards the coast at an arbitrary water depth (denoted by subscript

m), and g is the acceleration due to gravity (m/s^2). The variable λ is introduced to simplify the equation by substituting λ as:

$$\lambda = gH_b/C_m^2$$

Where, H_b is the wave height from breaking region. Wave phase speed, C_m is calculated as $gT/2\pi$ (m/s), in which T is the mean wave period.

This estimated breaker angle at the surfzone from the offshore DWRB data is considered uniform for the selected region. The remaining parameters – *i.e.*, the breaker wave height (H_b), and wave period needed for the estimation of longshore current velocity were obtained from the WTG measured data. These parameters were applied in the equations presented in Table 1, and the currents are compared with the results from the measured currents at C1, and C2. The breaker angle was calculated every 30 min, which was further interpolated every 20 min to correlate with the WTG data. The measured current data at 20 min interval was used to calculate the statistical prediction performance parameters.

Results and Discussion

From the current speed measurements carried out at C1 and C2 for four consecutive days, it can be inferred that there is no significant change in the current pattern observed in this region. The observed tide at this location is mixed semi-diurnal, and the observations were carried out during the spring tidal phase, wherein the maximum tidal range was 1.4 m. A gradual increase in current speed was observed simultaneously at C1 and C2 on the 23rd and 24th of January 2017. During flood tide, the maximum observed current speed of 0.17 m/s was observed at C1, whereas, at C2, the maximum current speed observed was 0.20 m/s (Fig. 2a & b). The prominent observation identified in this study is greater current speed relative to the maximum tidal range. However, the current speed at this location is diurnal (Fig. 2a & b) and increased during the flood tide at C1 and C2. Thus, it is evident that strong currents have prevailed during the large water column, so it is important to pay attention during rising tide phases for beach users. The foreshore slope estimated at C1 is 2.48°, and at C2, it is 2.8°, which implies that the increase in foreshore slope can increase the magnitude of the surfzone currents under prevailing conditions.

The current direction observed in this region varied promptly with the rise and fall in water level. Initially, on 21st January 2017, it was observed that flow

direction was moderately towards the southwest at C1 and northwest at C2, with the predominance of cross-shore currents (Fig. 2c). On 22nd January, during the ebb tide phase, dominant southward flow at C2 is followed by prevailing cross-shore currents at C1. Such significant cross-shore currents were abrupt during the ebb and flood tide phases with maximum tidal range. Moreover, the measurements revealed that the current direction at this location did not uniformly vary with the tidal phases and was predominantly towards the southwest and northwest directions.

At C2, when the tidal range is small (0.5 m), the flow persists as offshore flow, whereas during high tidal ranges (< 1 m) with ebb phases, the current direction is observed towards the south. Rip currents were observed in this region, which is predominant during the mid-tides and low tidal levels (Fig. 2c, circles). The flow patterns vary with the tide. At C1 and C2, a prominent feature was observed on the 22nd and 24th of January during the low tide. While the dominance of offshore flow was observed at C1 and the flow was predominantly in the alongshore direction towards the south at C2.

Significant wave height (H_s) at this location shows a decreasing trend during this study. The H_s decreased from 0.71 to 0.39 m from 21st January to 25th January 2017. A similar trend was observed for the H_s at DWRB data. There is a significant rise in H_s , observed during ebb tides on the 23rd and 24th of January. This study shows that rise and fall in H_s are observed at every diurnal cycle of the low tide whenever the tidal range becomes higher (Fig. 3a). The mean wave period T_m observed at this location was higher at the inner surfzone region than at the 15 m depth. T_m showed a diurnal variation with the prevailing semi-diurnal tide. Irrespective of H_s , the mean period increased from 21st to 25th January. Maximum T_m observed is 8 s at W1 and 5.5 s at 15 m depth (Fig. 3b).

The wave breaking angle, calculated based on Larson *et al.*²⁰, showed that the maximum breaking angle with the coastline was 0.78° (Fig. S1). Wave direction observed in this region did not show any major changes during the study and the waves were from the southwest direction. The meridional component of the wind ranges up to 6.7 m/s (Fig. S2), signifying a diurnal trend. Since, based on observations, the influence of H_s as well as T_m on the surfzone current variations could not be convincingly established, the role of other factors like the tide, foreshore slope, and wind parameters on the generation

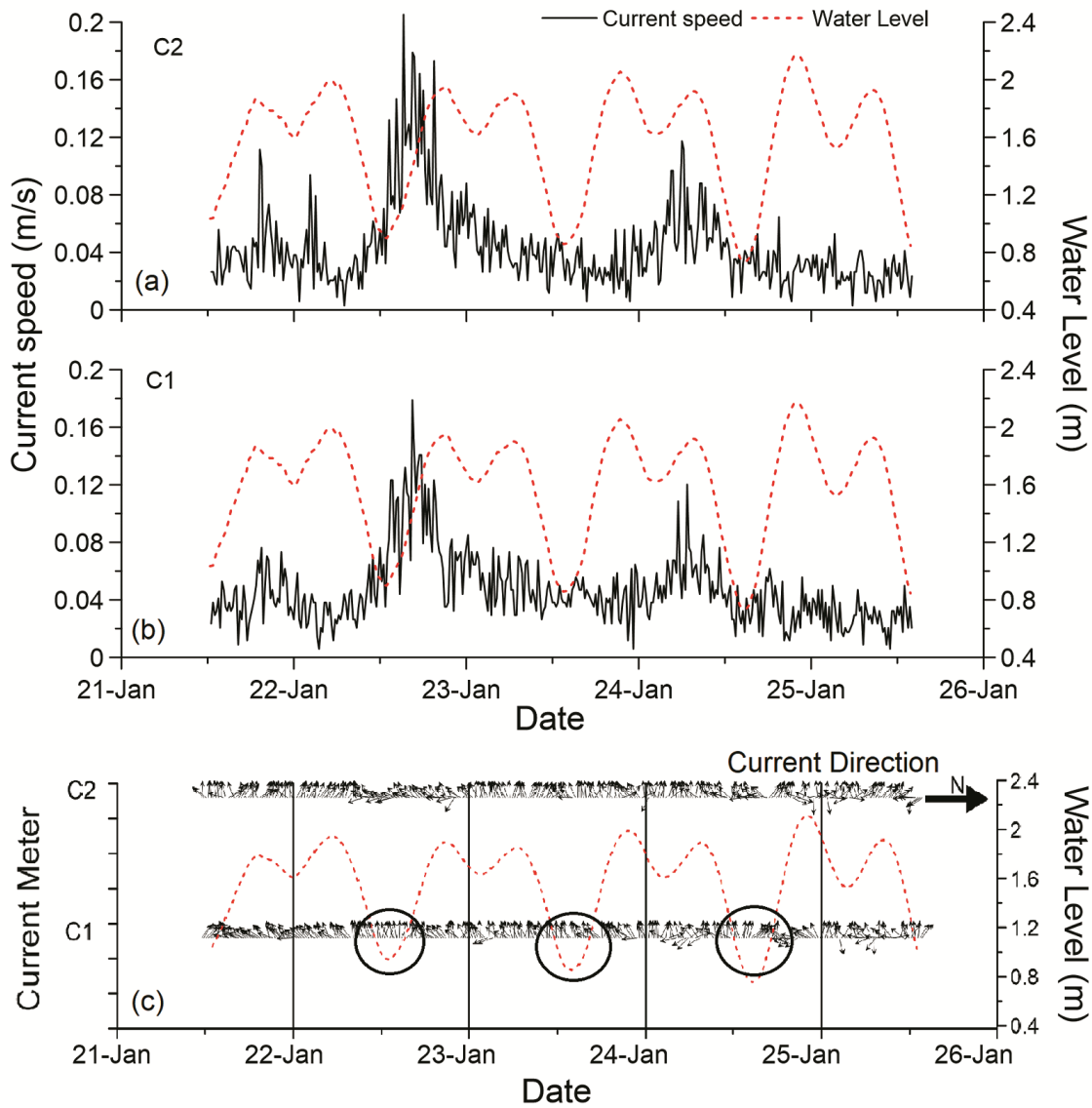


Fig. 2 — Alongshore varying current speed and current direction at Candolim with water level

of currents in the surfzone needs to be considered, and this is discussed in the following sections.

Case-1: Comparison of LSC velocity measurement vs estimated velocity by theoretical equations

The six LSC equations presented in Table 1 were considered to estimate the LSC velocity using the measured wave parameters from W1 and beach slope (Table 1). The estimated LSC velocity at C1 (with W1 as input) using the equation of IQ1 was overpredicted by four times (Fig. 4IQ1). The maximum LSC velocity estimated by IQ1 was 0.24 m/s; whereas, the maximum measured velocity at C1 is only 0.060 m/s. LSC estimation by HA1 is also overpredicted with a maximum speed of 0.19 m/s

which is almost 210 % greater than the measurements. Among these equations, estimations from the GA1 equation were 7 % lesser than the measured speed at C1. However, LH1, PMT1, and KO1 equations estimated lesser magnitudes by about 36, 51, and 86 %, respectively, with measurements.

The maximum LSC measured at C2 is 0.069 m/s, but estimated LSC shows that IQ1 and H1 overpredict the velocity with a maximum speed of 0.24 and 0.19 m/s, respectively (Fig. 5). The maximum LSC estimated by LH1 is 0.038 m/s, which is 45 % lesser than measurements at C2. GA1, KO1, and PMT1 underestimated the maximum LSC by 19, 88, and 57 %, respectively.

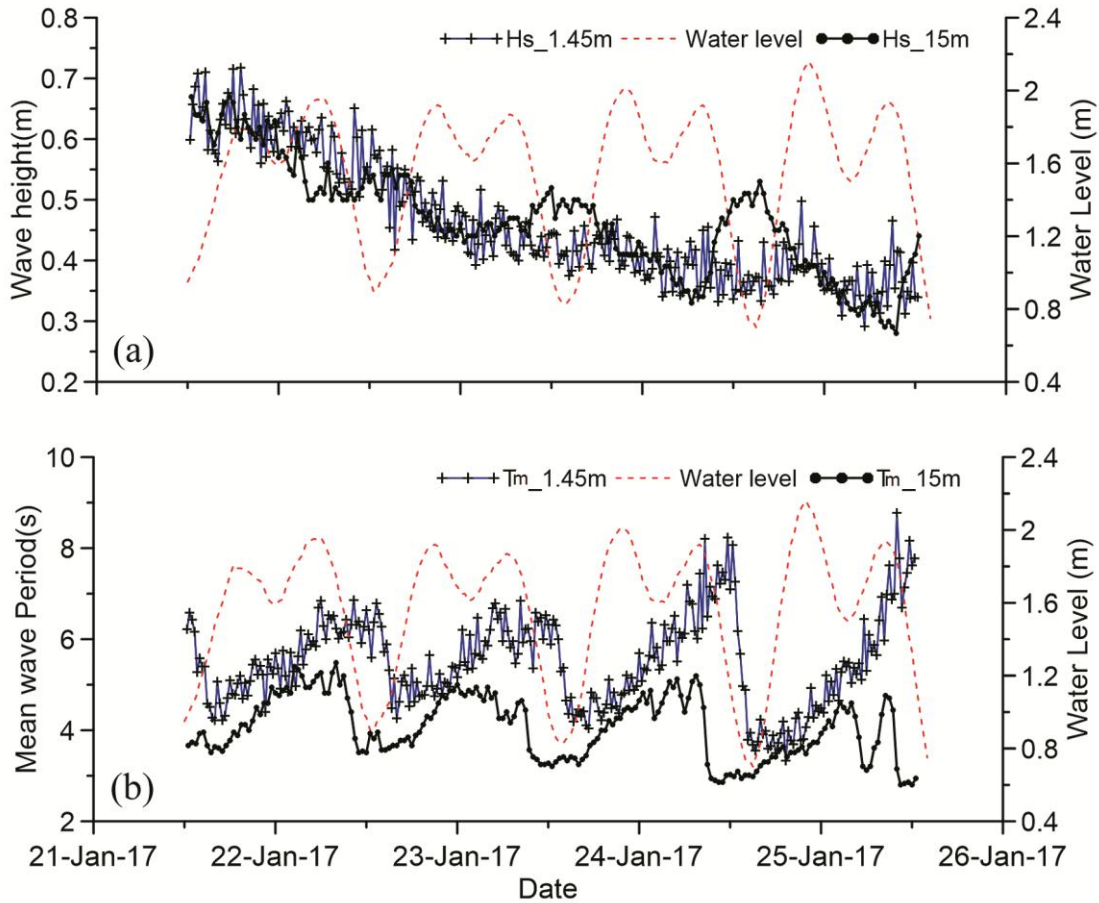


Fig. 3 — Alongshore varying significant wave height and mean wave period observed at surfzone of Candolim vs off Goa

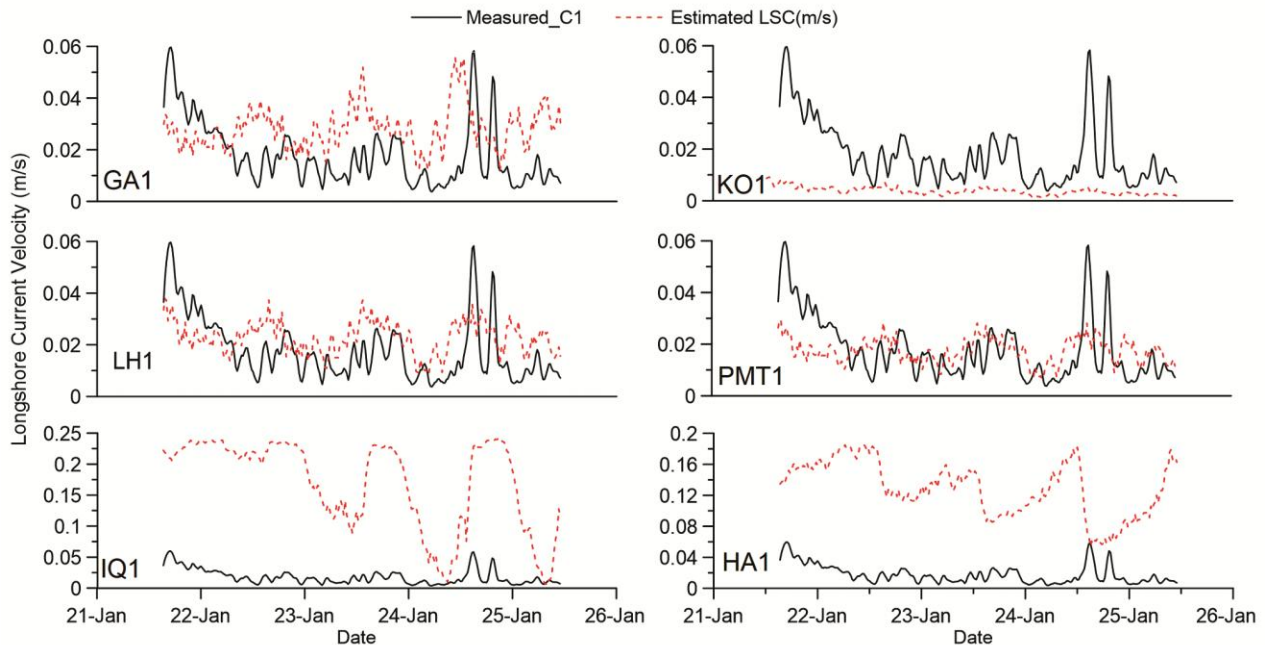


Fig. 4 — Comparison of estimated longshore current velocity with measurements at C1

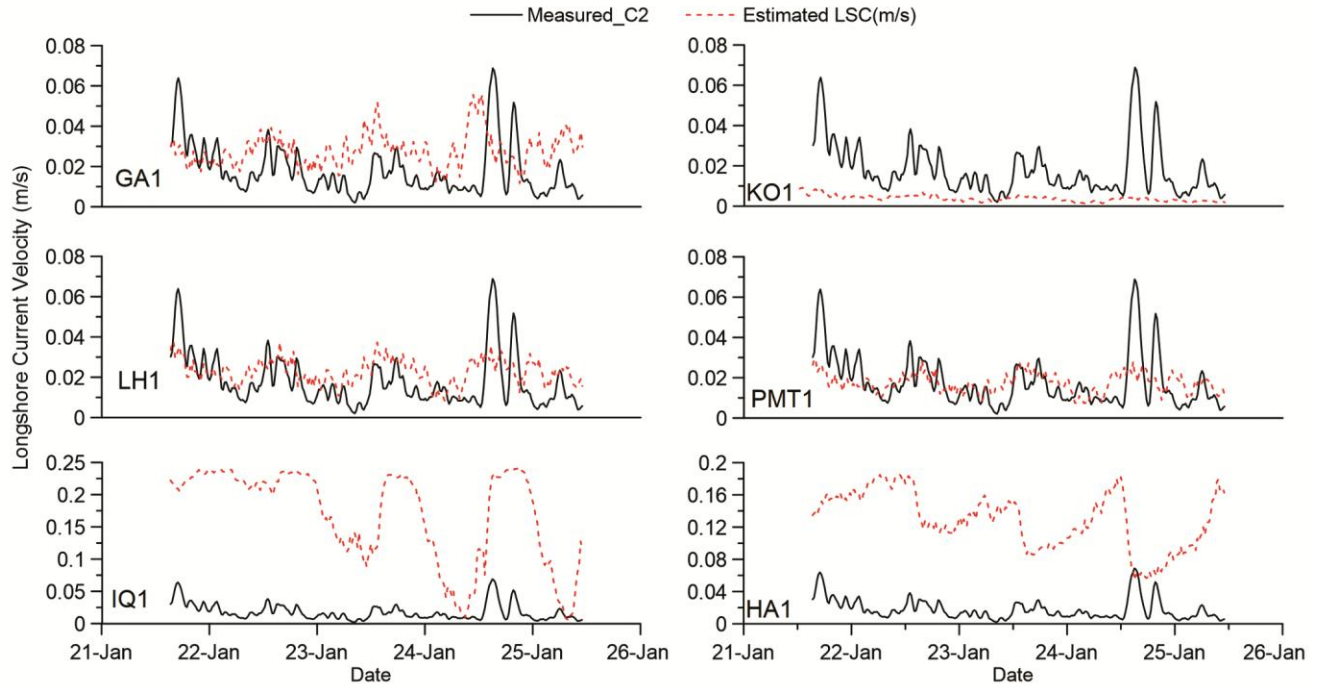


Fig. 5 — Comparison of estimated longshore current velocity with measurements at C2

Table 2 — Evaluating the performance of the equations for W1 data

Current meters	Scheme	GA1	LH1	IQ1	KO1	PMT1	HA1
C1	MAPE (%)	151.47	96.06	1106.79	72.73	66.37	973.20
	RMSE	0.02	0.01	0.17	0.02	0.01	0.12
	SI (%)	101.61	69.82	893.57	104.00	65.64	640.35
	R2	-0.03	0.43	0.49	0.65	0.42	0.10
C2	MAPE (%)	159.44	99.75	1166.28	72.76	68.47	1021.34
	RMSE	0.02	0.01	0.17	0.02	0.01	0.12
	SI (%)	101.56	73.22	863.07	110.01	71.67	619.57
	R2	0.05	0.49	0.41	0.64	0.49	0.02

In addition to general statistics, correlation and performance indices were calculated to evaluate the predictability of these equations. The evaluation was carried out based on four error estimation methods *viz.*, Mean Absolute Percentage Error (MAPE), Root Means Square Error (RMSE), Scatter Index (SI), and the correlation coefficient (*R*).

$$MAPE = \left[\frac{1}{N} \sum_{i=1}^N \left| \frac{P_i - O_i}{O_i} \right| \right] \times 100$$

$$RMSE = \sqrt{\frac{1}{N} \sum_{i=1}^N (P_i - O_i)^2}$$

$$SI = \frac{RMSE}{\bar{O}} \times 100$$

$$R = \frac{\sum_{i=1}^N (P_i - \bar{P})(O_i - \bar{O})}{\sqrt{\sum_{i=1}^N (P_i - \bar{P})^2 \sum_{i=1}^N (O_i - \bar{O})^2}}$$

Where, O_i is the observed value and P_i is the predicted value, N is the total number of points, \bar{O} is

the mean of the observations, and \bar{P} is the mean of the predicted values.

Estimated LSCs at C1 and C2 using the measurements at W1, gave large MAPE for all the equations. Correlations between LSC measurements at C1 and C2 were in good agreement with LH1, IQ1, KO1, and PMT1 (Table 2). However, GA1 and HA1 failed to give a good correlation with measurements. SI of the LH1 and PMT1 was better for C1 and C2. KO1 prediction showed a 64 – 65 % correlation with the measurements at C1 and C2, with a SI of more than 100 %. In this study, LH1 and PMT1 have been identified as better estimation methods with less percentage of error and better correlations with the measurements.

Still, these equations are intended to modify to obtain a much better results. Hence, a new term of alongshore wind speed observed off Goa is included

in all the equations. The LSC values estimated using the modified equations are discussed in case-2.

Case-2: Comparison of LSC velocity measurement vs estimated velocity by modified theoretical equations

The measured data set of Moore & Scholl²² included very low wave parameters that are not represented in any other study. They used an average H_b of 0.4 m, breaker angle θ_b ranging from $0^\circ - 5^\circ$, in this condition, it is possible that other physical parameters can have more influence on longshore current velocity. The results obtained from the field measurements from Candolim also satisfy the observations of Moore & Scholl²². In this study, the wave height measured from the surfzone ranged from 0.3 - 0.7 m, and the estimated breaker angle was less than 5° . Lanfredi & Framinan¹² identified the significance of the longshore component of the wind (Wu) in estimating LSC velocity.

They found that the influence of Wu is maximum during the summer and least during the winter and fall. Nummedal & Finley¹³ reported that a combination of Wu with the $\sin \alpha_b$ could influence the prediction of LSC more than breaking height and period. Hence in this study, Wu term is included in the existing equations as a function of $b_0 \times Wu$, where, b_0 is a constant taken as 0.1. The modified equations are given in Table 3.

The temporal variations of estimated LSC along the study area improved after modifying the equations (Table 3) along the study area. The estimated currents using most of the modified equations were within the range of the measured LSC speed. Significant rise

and fall observed in the current speeds at C1 and C2 were reflected in the estimations after the modifications (Figs. 6 & 7). At C1 and C2, for the LSC estimation using HA1, the maximum RMSE obtained was 0.12 for Case 1, and after the modifications (HA2), RMSE reduced to 0.01. Similarly, by using the modified IQ2 (Case-2), the RMSE, which was 0.17 for Case 1 (IQ1), was reduced to 0.04. Correlation between the estimated and measured currents also improved after the modifications. Further, the comparison of the estimated LSC using the measured data from W1 with the recorded current speed at C1 and C2 showed a reasonably good correlation of more than 55 % for all the equations.

Among that, LH2 and KO2 have a very good correlation of 65 % with measurements in C1 and 68 % with C2 (Table 4). GA2 has a 57 to 61 % correlation with C1 and C2, which is improved from a correlation of less than 1 %. Similarly, IQ2 also shows a better correlation of 61 % with C1 and C2 and its correlation is improved from 41 % after the modifications. PMT2 showed 57 to 61 % correlations for C1 and C2, which also improved from 42 % and 49 %. HA2 showed a 65 to 68 % of better correlation with the measurements at C1 and C2, which is far improved than case 1. MAPE is also improved after the modifications, especially for GA2, IQ2, and HA2. Reduction in MAPE value implies improvements in the prediction accuracy of the estimated method. Hence, all the six equations' performance was well improved after the modifications, especially for GA2,

Table 3 — Modified theoretical and empirical formulas used in the study

ID	Author	Modified formulae	Parameters	The basic scheme of analysis
LH2	Longuet-Higgins modified ¹⁰	$V = (20.7 m (g H_b)^{\frac{1}{2}} \sin(2\alpha_b))b_0Wu$	m = slope	Momentum radiation stress
PMT2	Putnam, Munk & Traylor ³	$V = \left(\frac{a}{2} \left(\sqrt{1 - \frac{4C \sin \alpha}{a}} - 1 \right) \right) b_0Wu$ $a = (2.61H_b m \cos \alpha) / KT$	m = slope, K = 0.0078, breaking wave velocity $C = \sqrt{2.28gH_b}$	Momentum
IQ2	Inman and Quinn ⁸	$V = \left(\left[\frac{1}{4X^2} + C \sin(\alpha_b) \right]^{\frac{1}{2}} - \frac{1}{2X} \right)^2 b_0Wu$ $X = 108 * a * \frac{H_b}{T_b} m \cos \alpha_b$	$C = \sqrt{2.28gH_b}$	Momentum
KO2	Komar ¹¹	$V = (20U_m \sin \alpha_b \cos \alpha_b b_0)Wu$ $U_m = \frac{1}{2} \gamma_b (gH_b)^{1/2}$	U_m = Maximum wave orbital velocity $\gamma_b = 0.46$	Empirical
GA2	Galvin ⁶	$V = KgmT \sin(2 \alpha_b) b_0Wu$	K = 1	Continuity
HA2	Harrison ⁹	$\bar{v} = ((-0.215 + 0.0317376(\overline{\alpha_b}) + 0.031801(\overline{T_b}) + 0.241176(H_{bs}) + 0.030923(\overline{m}))b_0Wu$	\bar{m} is slope	Multiple regression

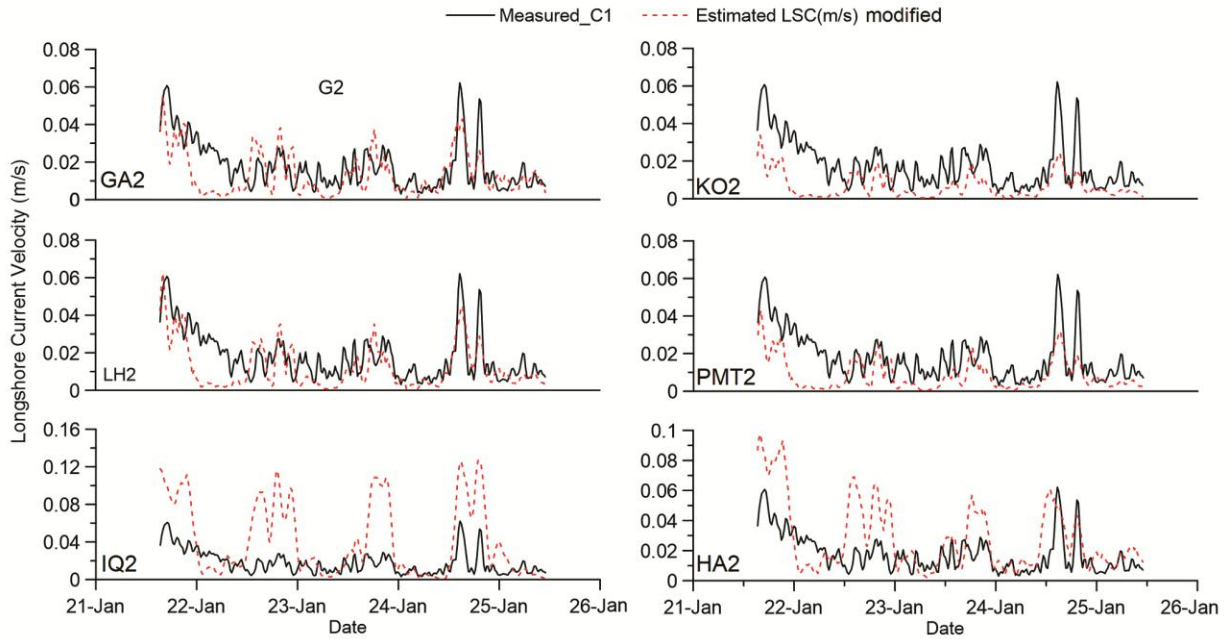


Fig. 6 — Comparison of estimated longshore current velocity using modified equations with the measured current at C1

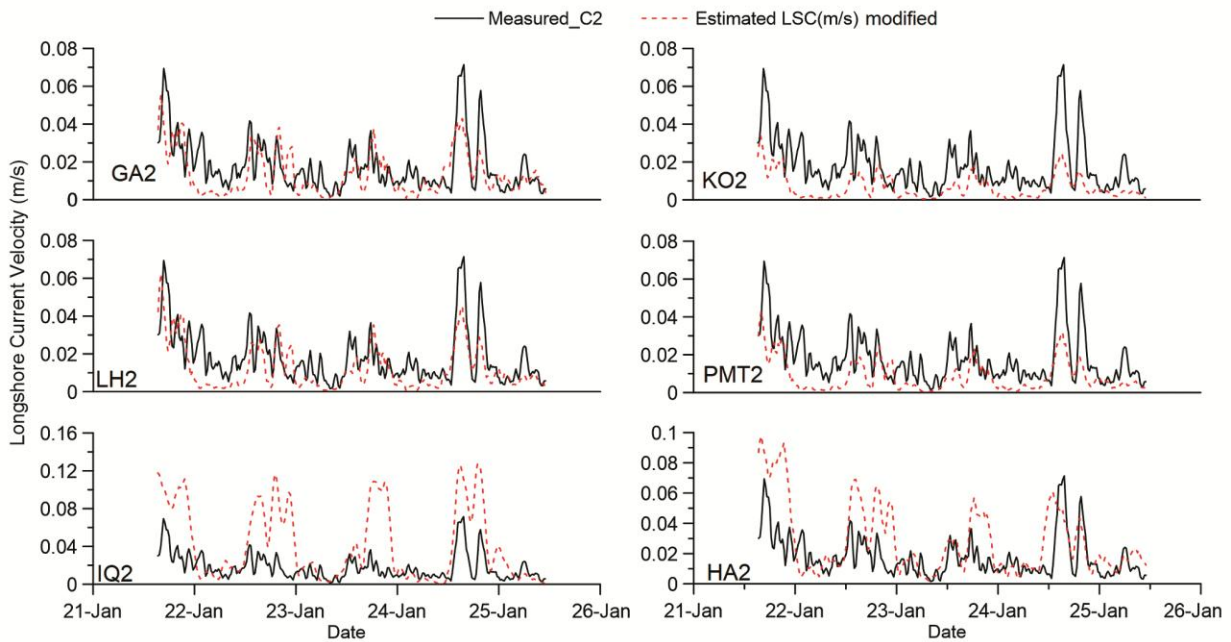


Fig. 7 — Comparison of estimated longshore current velocity using modified equations with the measured current at C2

Table 4 — Evaluating the performance of the equation after modifications for W1 data

Current meters	Scheme	GA2	LH2	IQ2	KO2	PMT2	HA2
C1	MAPE (%)	61.83	58.68	196.34	64.77	61.83	58.7
	RMSE	0.01	0.01	0.04	0.01	0.01	0.01
	SI (%)	67.53	65.59	229.5	83.61	67.53	65.6
	R2	0.57	0.65	0.61	0.65	0.57	0.65
C2	MAPE (%)	60.93	58.07	195.43	64.06	60.93	58.1
	RMSE	0.01	0.01	0.04	0.02	0.01	0.01
	SI (%)	67.44	66.64	225.08	86.58	67.44	66.6
	R2	0.61	0.68	0.61	0.68	0.61	0.68

IQ2 and HA2. Even after the modifications, it implies that LH2, KO2, and PMT2 are better estimation methods and can be used for the estimation of LSC velocity than other equations.

Conclusions

The measured current speed at Candolim C2 varied between 0.04 and 0.16 m/s, and the current direction indicated the predominant occurrence of rip currents at this location, particularly during the low and mid tides. Rip currents were observed prominently in this area with higher intensity during the ebb tide. Laboratory experiments of Galvin & Eagleson⁶ also stated that longshore currents were maximum between the still water line (Initially) on the beach and the breaker region. However, under a particular environment, longshore currents may turn seaward into a rip-like current. The observed current speed is not consistent along the Candolim Beach; it is found that current speed at C1 is more than C2. The rise in current speed is observed during the ebb tide at C1, and it is evident that when the current speed increases, the wave period decreases significantly. The maximum wave period was observed on 24th January during the ebb tide. The foreshore slope plays a prominent role in varying the current magnitudes at C1, and C2. It is observed that the current speed increased with the foreshore slope at C2. However, this similarity is not seen while estimating the LSC speed using the theoretical equations. The LSC estimated using the equations showed a wide range of MAPE and SI in this study.

Correlation is also restricted within the range of 50 % achieved by the equations of Longuet-Higgins (LH1) modified by CERC, Komar (KO1) and Putnam, Munk and Traylor (PMT1). A modification is employed to increase these six equations' predictive performance by introducing an alongshore component of wind velocity (Wu). After the modification, the estimation of the LSC by these equations was improved, especially before modification Galvin (GA1), Inman *et al.* (IQ1) and Harrison (HA1) overpredicted the LSC velocities by a large margin. The modified equations have accurately estimated the rise and fall in the LSC at C1, C2. The Correlation coefficients also improved up to 68 % for LH2, KO2 and HA2 equations as an earlier study by Yadhunath *et al.*¹⁷ identified that modified Longuet-Higgins and Komar equations are predicting better results. In this study, based on statistical analysis, modified

equations of Longuet-Higgins, Komar, and Putnam *et al.*, predict the LSC speed with higher accuracy. Existing standard equations by Longuet-Higgins and Komar estimated longshore currents at C1 and C2 better than the earlier study wherein a single point current measurements within a span of 2 h was used. Modification in LSC estimation after introducing the alongshore component of wind was well established in this study, which further needs to be considered in the estimation of longshore currents.

Supplementary Data

Supplementary data associated with this article is available in the electronic form at [https://nopr.niscpr.res.in/jinfo/ijms/IJMS_51\(11\)867-877_SupplData.pdf](https://nopr.niscpr.res.in/jinfo/ijms/IJMS_51(11)867-877_SupplData.pdf)

Acknowledgements

The authors acknowledge the facilities and support provided by CSIR-National Institute of Oceanography. This manuscript is part of PhD work of the first author. This manuscript has NIO Contribution number 7092.

Conflict of Interest

There is no conflict of interest.

Funding

CSIR – NIO contributed a majority of the funding for salaries and equipment. Part funding is provided by the Ministry of Earth Sciences through project sanction no. MoES/36/OOIS/Extra/4/2013dt.20/10/2014.

Author Contributions

JKS conceptualized the work, contributed to data collection and analysis, and in manuscript editing and finalizing. YEM carried out the field measurements, data collection and analysis and prepared the manuscript. PSP, RK, and RG contributed to the field measurements for data collection.

References

- 1 Reniers A & Battjes J, A laboratory study of longshore currents over barred and non-barred beaches, *Coast Eng*, 30 (1) (1997) 1-21.
- 2 Guza R & Thornton E, Variability of longshore currents, *Coast Eng Proc*, 1 (16) (1978) p. 43. DOI: <https://doi.org/10.9753/icce.v16.43>
- 3 Putnam J A, Munk W H & Taylor M A, The prediction of longshore currents, *Trans Am Geophys Union*, 30 (1949) 337-345.
- 4 Saville T, Model studies of sand transport along an infinitely straight beach, *Trans Am Geophys Union*, (31) (1950) 555-556.

- 5 Brebner A & Kamphuis J W, Model tests on the relationship between deep water wave characteristics and Longshore currents, *Coast Eng*, (9) (1964) 191-196.
- 6 Galvin C J & Eagleson P S, *Experimental study of longshore currents on a plane beach*, (US Army Coastal Engineering Research Center, Washington D C), 1965, pp. 198. <https://apps.dtic.mil/sti/pdfs/ADA345211.pdf>
- 7 Galvin, *Experimental and theoretical study of longshore currents on a planar beach*, Ph.D. Thesis submitted to Department of Geology and Geophysics, Massachusetts Institute of Technology, Cambridge, 1963, pp. 185. <http://hdl.handle.net/1721.1/58355>
- 8 Inman D & Quinn W, Currents in the surf zone, *Coast Eng Proc*, 1 (2) (1951) p. 3. <https://doi.org/10.9753/icce.v2.3>
- 9 Harrison W, Empirical equation for longshore current velocity, *J Geophys Res*, 73 (22) (1968) 6929-6936.
- 10 Longuet-Higgins, Longshore currents generated by obliquely incident sea waves: 2, *J Geophys Res*, 75 (33) (1970) 6790-6801.
- 11 Komar P D & Inman D L, Longshore sand transport on beaches, *J Geophys Res*, 75 (30) (1970) 5914-5927.
- 12 Lanfredi N W & Framiñan M B, Field Study and Prediction of Longshore Currents, Argentine Coast, *J Coast Res*, 2 (4) (1986) 09-417.
- 13 Nummedal D & Finley R J, Wind-generated longshore currents, *Coast Eng Proc*, 1 (16) (1978) 1428-1438.
- 14 Hanes D M, Longshore Currents, In: *Treatise on Geomorphology*, 2nd edn, edited by John F S, (Academic Press, Elsevier), 2022, pp. 83-99
- 15 Kumar V S, Chandramohan P, Kumar K A, Gowthaman R & Pednekar P, Longshore currents and sediment transport along Kannirajapuram Coast, Tamilnadu, India, *J Coast Res*, 16 (2) (2000) 247-254.
- 16 Hameed Shahul T S, Baba M & Thomas K V, Computation of Longshore currents, *Indian J Geo-Mar Sci*, 15 (2) (1986) 92-95.
- 17 Chandramohan P, Nayak B U, Anand N M & Sanil Kumar V, Field measurement on longshore current variation between Ratnagiri and Mangalore, west coast of India, In: *Proceedings of Eighth Conference of International Association of Hydraulic Research*, CWPRS, Pune, 1992, pp. 271-282.
- 18 Yadhunath E M, Jayakumar S, Jishad M, Gowthaman R, Rajasekaran C, *et al.*, Surfzone currents at Candolim and Miramar beaches of Goa, India: measurements and comparisons, *Indian J Geo-Mar Sci*, 43 (7) (2014) 1210-1216.
- 19 Chandramohan P, Sanil Kumar V & Jena B K, Rip current zones along beaches in Goa, west coast of India, *ASCE J Waterw Port Coast Ocean Eng*, 123 (6) (1997) 322-328.
- 20 Antony M, Wave refraction off Calangute beach, Goa, with special reference to sediment transport and rip currents, *Indian J Geo-Mar Sci*, 5 (1976) 1-8.
- 21 Larson M, Hoan L X & Hanson H, Direct Formula to Compute Wave Height and Angle at Incipient Breaking, *J Waterw Port Coast Ocean Eng*, 136 (2) (2010) 119-122.
- 22 Moore G W & Scholl D W, *Coastal sedimentation in northwestern Alaska*, (US Atomic Energy Commission, TEI No. 779), 1961, pp. 43-65.